Construction and Building Materials 102 (2016) 1018–1028

Contents lists available at ScienceDirect

Construction and Building Materials

journal homepage: www.elsevier.com/locate/conbuildmat

On the delamination phenomenon in the repair of timber beams with steel plates

Giovanni Metelli *, Marco Preti, Ezio Giuriani

Department of Civil, Environmental, Architectural Engineering and of Mathematics, University of Brescia, Italy

HIGHLIGHTS

- A non-invasive technique for the repair of ancient wooden floors is presented.
- Steel plated were glued on one side into longitudinal routed grooves.
- The plate delamination was studied with the Moiré interferometry analysis.
- The plastic strain of sapwood markedly reduced the risk of delamination.
- The continuous monitoring of the floor confirms the effectiveness of the technique.

ARTICLE INFO

Article history:
Received 14 January 2015
Received in revised form 5 September 2015
Accepted 21 September 2015
Available online 1 October 2015

Keywords:
Timber
Repair
Delamination
Stress concentration
Bond
Interferometry analysis
Creep

ABSTRACT

This paper presents a non-invasive technique for the repair of ancient wooden floors. Steel plates are glued on one side only by epoxy-adhesive into longitudinal grooves in order to allow the free swelling and shrinkage of the wood in the direction transversal to the plate glueing surface, thus reducing the risk of plate delamination. A set of high strength steel nails provides load transmission from the steel plates to the wooden beam in the case of loss of adhesion due to fire or delamination. This technique was used to repair a precious beam in a 15th-century wooden floor in Palazzo Calini (Brescia, Italy). The technique requires particular attention because it might be affected by the delamination of the glued reinforcement due to stress concentration, which occurs at the end of the repairing element or at any cracks in the repaired beam. Results of experimental studies on delamination phenomenon investigated by means of the Moiré interferometry analysis are also presented. These show that the risk of plate debonding can be markedly reduced by the capability of the sapwood to develop plastic strain. The wooden floor has been monitored for more than fourteen years, confirming the effectiveness of the adopted technique.

1. Introduction

In the rehabilitation of ancient buildings the problem of strengthening and repairing wooden beams is encountered often. In recent years, theoretical, numerical and experimental studies have been carried out to find valid techniques to enhance the stiffness and the strength of ancient wooden floors. These techniques are essentially based on the use of thin collaborating concrete slab or steel plates [1,2]. Several techniques have been developed since the 1960s, which are especially focused on strengthening and repairing local fractures or defects in wooden beams with steel plates bonded by epoxy adhesive [3–6]. More recently, fibre-reinforced polymer (FRP) sheets have been proposed to replace steel plates because they are easily installed and provide good durability [7–11]. Generally these techniques require wide steel plates or FRP strips which cover a large part of the surface of the wooden beam. This aspect makes it difficult to apply these techniques to the repair of precious ancient wooden floors.

The restoration technique proposed by Gentile et al. [12], Alhayek and Secova [13] and by Alam et al. [14] seems to be more acceptable. It uses glass-fibre (GFRP) or carbon-fibre reinforced polymer (CFRP) reinforcements that were glued into narrow longitudinal grooves routed out of the wood beam. This limits the intervention to a reduced portion of the beam, which remains mostly visible. This technique was adopted to efficiently strengthen 75 timber beams of a bridge in Canada [12]. All of the previously mentioned techniques, based on the collaboration between two elements of different materials, pose the issue of stresses occurring between the reinforcing element and the wood, induced by the

* Corresponding author at: DICATAM, University of Brescia, via Branze 43, Brescia, Italy.
E-mail address: giovanni.metelli@unibs.it (G. Metelli).

http://dx.doi.org/10.1016/j.conbuildmat.2015.09.038
0950-0618/

wood's swelling and shrinkage resulting from its cyclic changes in moisture content.

Another important issue raised by these reinforcing techniques concerns the risk of delamination, as the collaboration between the two materials – steel and timber – results in a concentration of normal and shear stresses induced by a discontinuity of one of the two elements (Fig. 1). Two brittle failure modes characterise the debonding from timber of adhesively-bonded plates: delamination might occur (i) at the cut-off point of the plate, propagating inward along the beam (end peeling) or (ii) at the toe of transversal fractures of the repaired beam and it moves toward the plate ends (midspan debonding) (Fig. 2). In recent years, these phenomena have been widely studied but specifically for reinforced concrete beams strengthened with steel plates [15,16] or with plastic reinforcements (FRP) [17,18]. These experimental studies showed that the strength and the stiffness of the beam can be substantially increased with the modulus and the amount of the applied reinforcements. However, the effectiveness of the technique may be impaired by plate delamination, which mainly depends on the characteristics of the concrete cover, shear span of the beam and on the extension of the bonded plates. Moreover, the research studies of Rahimi and Hutchinson [17] and of Sebastian [18] pointed out that the use of thin plates may encourage midspan debonding rather than end peel action in a plated beam.

Several numerical [19,20] and analytical [20–22] research studies were also carried out. Although all these theoretical studies have shed light on interface stress concentrations, they do not interpret real local diffusive effects because they assume a linear elastic behaviour of the connected materials. It should be noted that few numerical studies take into account non-linear constitutive relationships for the plate-concrete bonding interface to model concrete beams strengthened with bonded FRP reinforcement [23,24], thus allowing for a mitigation of the stress concentration. Despite the several experimental studies which show the effectiveness of steel or CFRP reinforcement to strengthen [12,13] or repair fractured timber beams [15], few specific investigations aimed at studying the delamination phenomenon are available in the literature [4,5].

In this paper a repair technique adopting steel reinforcing elements glued into grooves is presented with particular devices to avoid both the risk of the interface splitting due to the wood swelling and shrinkage, and the risk of collapse due to the delamination of the repairing element induced by peak stress. This technique was used to repair an ancient beam in a 15th-century wooden floor in Palazzo Calini (Brescia) which has also been monitored for more than fourteen years since the repair. Results of experimental studies focusing on the delamination induced by stress concentrations and investigated by means of the Moiré interferometry analysis are also presented. This experimental campaign was carried out with the specific aim of understanding the role of the local shear behaviour of sapwood in the onset of plate debonding.

2. Degradation assessment of a fifteenth-century beam

The repair was carried out on a larch main beam of a fifteenth-century wooden floor in "Palazzo Calini ai Fiumi" (Brescia, Italy). The beam is 220 mm wide, 500 mm deep with a 7.5 m clear span. The distance between the main floor beam centres varies between 3.2 and 3.7 m. These support the secondary beams (110 mm wide and 150 mm deep) with a spacing of about 0.55 m (Fig. 3). It should be noted that the beams of Palazzo Calini are covered by an ancient and precious paint, which does not allow a clearly defined classification of the timber as it may be done for new elements. However, on the basis of a visual grading of the dimension of main knots, the characteristic bending strength should be about 20 MPa as suggested by Italian standard for larch [25].

On 1997 the floor was stiffened by replacing the original lime-mortar slab with a 50 mm thick collaborating concrete slab

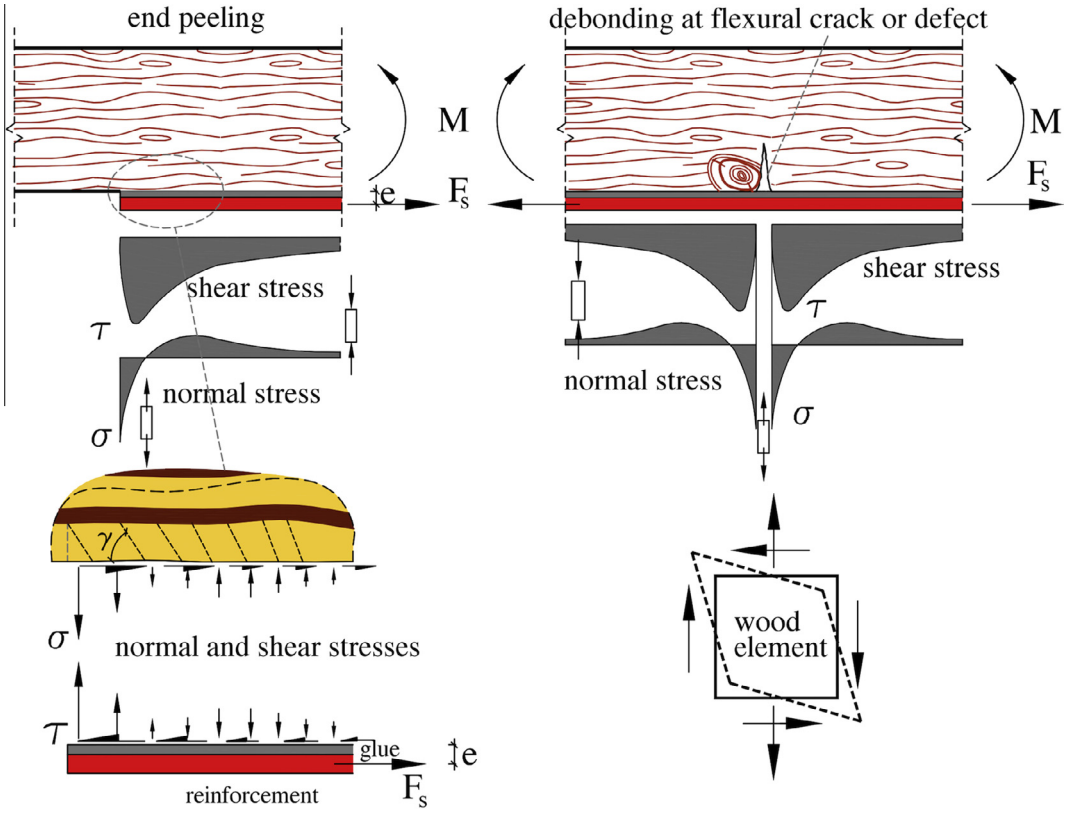

Fig. 1. Stress concentration at plate ends or close to beam defects.

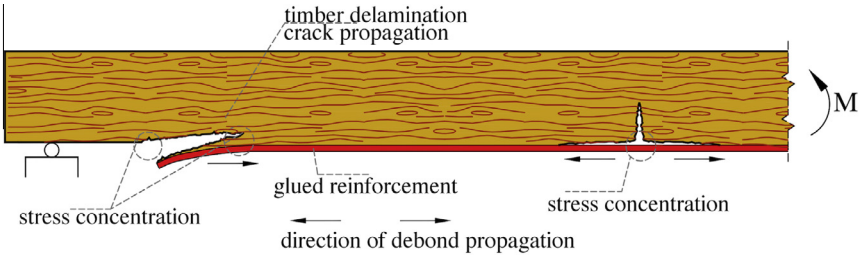

Fig. 2. Delamination of the timber near the glueing surface at plate ends or at midspan close to defects and cracks.

Fig. 3. Wooden floor of "Palazzo Calini ai Fiumi" before the repair (Brescia – Italy).

(C25/30 class), connected to the wooden beams by means of steel studs (16 mm diameter with a spacing varying from 75 mm at supports and 150 mm at midspan) [1]. This strengthening work was designed by assuming a characteristic value of structural dead loads G_{k1} = 1.85 kN/m^2, of non-structural dead loads G_{k2} = 1.00 kN/m^2, and a characteristic value of the variable loads Q_k equal to 3.0 kN/m^2 [26]. It should be noted that the intervention was carried out without any propping of the wooden floor during concrete curing, thus resulting in high timber stress under service condition which is equal to $\sigma_{w,s}$ = 6.3 MPa for permanent loads only ($\sigma_{w,s}$ = 9.0 MPa for a rare combination of actions). Before the intervention the timber floor sustained a dead load of only 1.2 kN/m^2 which determined a lower timber stress of 3.4 MPa.

On 2000 it was observed that one of the main beams (labelled TA-R in Fig. 3) was characterised by a large deflection equal to 70 mm ($\approx L/100$), caused by the formation of dangerous (60 mm deep) transversal cracks originating from a large knot located at the midspan soffit (Fig. 4). The deflection of the adjacent main beams was markedly lower at about L/180, thus showing overall good conservation of the ancient floor. A wide transversal crack (A in Fig. 4a and c) spread from a large wooden knot placed at the beam section soffit to the beam side joining a longitudinal crack on the beam side. A second severe crack (B in Fig. 4a and c) developed from the same knot with a depth of close to 60 mm and joined a second significant transversal crack (C in Fig. 4a and c). A third longitudinal crack (D in Fig. 4), originating from a second knot, characterised the southern side of the beam at a distance of about 2 m from the support. The crack pattern is also depicted in Fig. 4c.

In order to evaluate and choose the most appropriate restoration technique for the damaged beam, the wood decay was assessed by means of in-situ penetration tests. These tests consist in the measurement of the penetration of a graduated rod, which advances by means of repeated blows of a rebound hammer [27]. This technique makes it possible to distinguish between different degrees of decay as a function of the number of blows necessary for 1 cm penetration. The assessment is possible by means of correlation curves between the number of blows and the strength of the wood according to the wood species, moisture content and the penetration direction with respect to the grain direction [27]. This technique was proposed and adopted for an extensive investigation of the wood truss-arches of the roof vault of the "Palazzo della Loggia", a 15th century building in Brescia (Italy). It gave useful indications of the extent and depth of the decay of the wooden structure.

With regard to the damaged beam of the wooden floor in Palazzo Calini (Brescia), several tests were performed up to a penetration depth of 40 mm with the number of blows for 1 cm of penetration varying between 6 and 12. The beam moisture content ranged between 9.5% and 10%. As a result, the in-situ

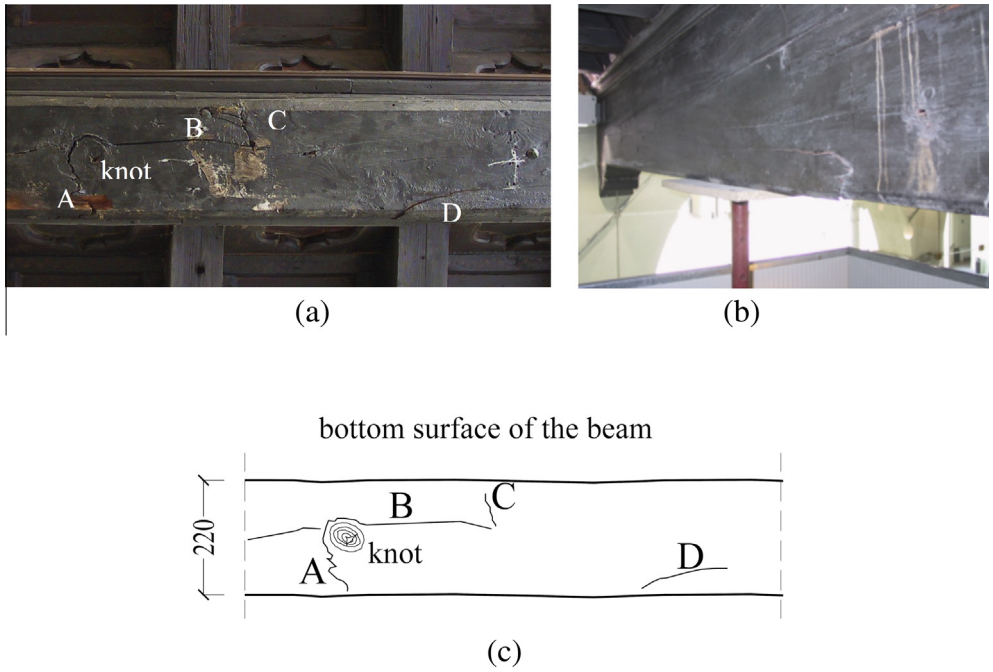

Fig. 4. Details of splitting cracks at the beam soffit (a), on the beam's southern side (b) and crack pattern on the beam's bottom surface (c).

penetration tests on the beam of the Palazzo Calini showed its good conservation with an absence of wood decay, thus confirming the possibility of the beam repair limited to the splitting cracks at the beam midspan.

3. Repair technique

The fifteenth-century timber beam was repaired on 2001 with steel plates glued to the timber with epoxy-resin adhesive (Fig. 5a). The grooves had a limited width of 16 mm and a depth that varied from 60 mm at the midspan to 0 mm at the groove ends in order to minimise wood removal. On each side of the groove a 4 mm thick steel plate was glued leaving a clearance of about 5 mm between the two steel plates (Fig. 5b). The mechanical properties of the epoxy-adhesive are listed in Table 1.

Moreover, it is worth noting that this technical device, using steel plates glued on one side only into internal grooves, reduces the risk of the delamination of the plates caused by the swelling and shrinkage of the wood, from cyclic moisture content variations, while not producing additional stresses on the glued surfaces. If the steel plates had been glued on both sides into routed slots, as widely proposed in the literature [3,6,11–14], the deformation of the wood, induced by the moisture content variations, would have produced cyclic compressive and tensile stresses perpendicular to the glued surfaces, which might have caused their failure by splitting. Furthermore, unlike the repair technique with external plates glued to the beam's sides or to the bottom surface [6–11], the choice of internal steel plates allows the epoxy-adhesive layer to be protected in case of fire by applying a longitudinal wooden strip, which covers the groove.

The six steel plates (4 mm thick, 50 mm deep and 4.2 m long – S275 grade steel having a nominal yield strength f_{yk} = 275 MPa) were designed to guarantee an adequate strength and stiffness to the repaired beam. The design criteria for these reinforcements is based on the assumption that they carry the tensile action corresponding to the cracked portion of the timber section with a steel stress (σ_s) of 100 MPa at service loading:

$$A_s > A_{s,min} = (\sigma_{w,s} b d_{cr})/(n_p \sigma_s) = 198 \text{ mm}^2 \quad (1)$$

being A_s = 200 mm^2 the cross section of each steel plate, b = 220 mm the beam width, d_{cr} = 60 mm the depth of the cracked section, n_p = 6 the number of steel plates and $\sigma_{w,s}$ = 9.0 MPa the maximum tensile stress in the timber for the rare combination of actions at serviceability limit state ($G_{k1} + G_{k2} + Q_k$). The bending resistance of the composite section (M_{Rd}), calculated by assuming a propagation of defects and cracks within the timber section, is greater than the bending action (M_{Ed}) at ultimate limit state, as shown by the following equations:

$$M_{Rd} \approx n_p F_{yd} z = 300 \text{ kN } 0.67 \text{ m} = 201 \text{ kN m} \quad (2)$$

$$F_{yd} = A_s f_{yk}/\gamma_{M0} = 50 \text{ kN} \quad (3)$$

where (F_{yd}) is the design axial strength of each plate, and z = 0.67 m the internal lever arm, and γ_{M0} = 1.10 the partial safety factor for steel. It should be noted that the bending action was evaluated by assuming beam span L = 7.8 m, a distance between the main beam centres of 3.45 m and that the construction process was adequately controlled (safety partial factor of permanent action γ_G = 1.05 and of variable action γ_Q = 1.5 [28]):

$$M_{Ed} = 197 \text{ kN m} \quad (4)$$

The bond length (l_b = 750 mm in Fig. 5) of the steel plates was selected to ensure the design axial strength (F_{yd}) of the reinforcements, given by Eq. (3), to be transferred to the undamaged zone of the timber beam. A uniform distribution of shear stresses was assumed along the bond length, as given by the following expression:

$$A_b f_{vd} > F_{yd} \quad (5)$$

where A_b = 2.5 × 10^4 mm^2 is the bond area and $f_{vd} = k_{mod} f_{vd}/\gamma_M$ = 0.9 3.4/1.3 = 2.3 MPa is the design shear resistance of Italian solid larch timber (class S3 according to Italian standard UNI 11035-2 [25]) for service class 1 and 2 and short term action of loads (EN1995-1-1:2004 [29]). The assumed value of the design shear resistance of the glueing surface has been confirmed by the results of several shear bond tests carried out at the P. Pisa Laboratory of the University of Brescia, as also discussed in Section 4.2 below. These

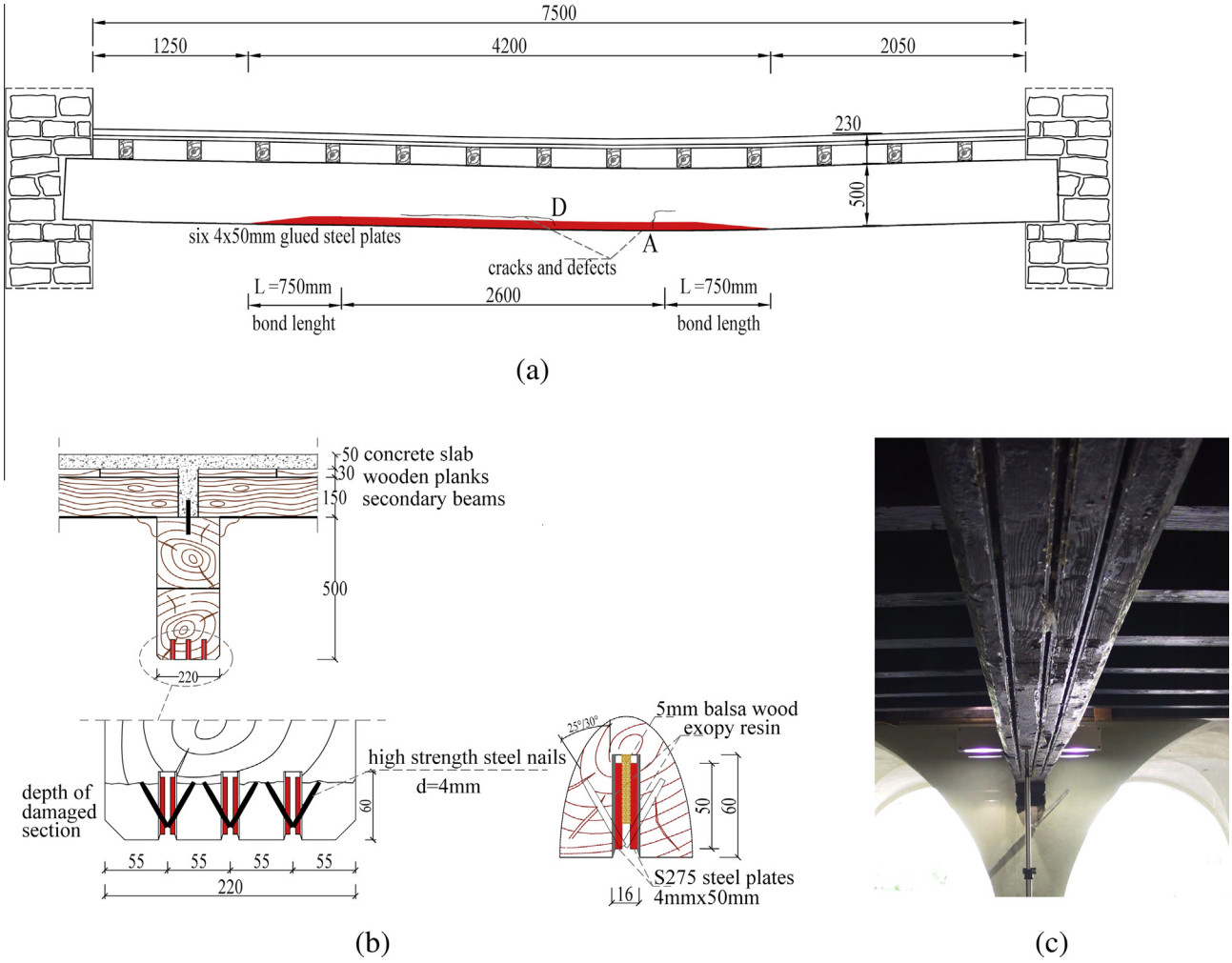

Fig. 5. Repaired beam of Palazzo Calini ai Fiumi (Brescia, Italy): beam deflection and crack pattern on the beam's south side (a); repaired cross section (b); soffit surface with the longitudinal glued steel plates (c).

Table 1
Main properties of the epoxy-adhesive at 20 °C.

Density	[kg/m^3]	1500
Young's modulus	[GPa]	>5.5
Tensile strength	[MPa]	24
Compressive strength	[MPa]	70
Adhesion on steel	[MPa]	21
Adhesion on concrete	[MPa]	4
Poisson's ratio	[–]	0.3
Coefficient of thermal expansion	[10^{-5}/C]	6.1

experimental results showed a bond strength greater than 5.0 MPa without any peeling failure of the steel-adhesive or wood-adhesive interface of the specimens [30,31]. The shear failure surface occurred in the early wood layer of each specimen thus confirming the efficacy of the epoxy-resin adhesive adopted and the reliability of the surface preparation before gluing.

Furthermore, a set of high strength steel nails (diameter 4 mm, length 60 mm, with 50 mm pitch) was also placed along the 0.75 m bond length of the steel plates (Fig. 5b and c). This nailed connection guarantees the transmission of the load from the steel plates to the wooden beam in case of loss of adhesion due to fire or delamination due to stress concentration. The nails were forced into calibrated holes (3.5 mm in the timber beam and 3.7 mm in the steel plates) made using a specific template. They were drilled at an alternating 25°/30° inclination with respect to the vertical axis of the beam section (Fig. 5b) to reduce the longitudinal splitting action of nails.

The nailed connections were designed by assuming plate debonding, as in the case of fire. Thus, the combinations of actions for accidental design situations was considered [28]:

$$\sum G_{ki} + A_d + \psi_{21} Q_k \tag{6}$$

being $\psi_{21} = 0.6$ in case of variable load of Category C2 (EN1991-1 [26]), for which the tensile stress in the plates of the repaired beam section is equal to $\sigma_s = 73$ MPa. In case of plate debonding, the tensile action of the plate is carried by the shear action on each nail, which is given by the following equation:

$$V_{Ed} = \sigma_s A_s / n = 0.97 \text{ kN} \tag{7}$$

being $A_s = 4 \times 50$ mm^2 the cross section of the plate and $n = 15$ the number of nails along the 750 mm bond length.

The characteristic shear resistance (V_{Rk}) of the steel-to-timber nailed connection may be efficiently evaluated by means of the main analytical models found in the literature [1,29,32,33] by assuming a nail strength $f_u = 800$ MPa, a timber density of $\rho_k = 620$ kg/m^3 [25], and by considering the formation of two plastic hinges in the nail shank (EN 1995-1-1:2004 [29]), as experimentally confirmed by preliminary tests [30]. The predicted connection strength is $V_{Rk} = 3.0$ kN which may guarantee a partial

safety factor (γ_M) of the connection greater than 3 in case of plate debonding due to fire. Preliminary tests carried out on nailed steel-to-timber connections showed a resistance of each shear plane of the fastener of about 2.75 kN [30], which agrees with the analytical results. These results also showed that the inclination of the nail axis with respect to the plate–timber interface did not impaired the connection strength since the shear action acts in the direction parallel to the wood grain.

With regard to the technological procedure of the proposed technique, Fig. 6 shows the main phases of the repair work. Firstly, tubular steel props were used to support the loads during beam repair (Fig 4b). Many props were erected at the secondary beam ends and at the main beam soffit to unload the damaged beam from the floor's dead loads before applying the reinforcements. These props were tightened to recover a beam deflection equal to 3 mm. Then, the three grooves were routed along the bottom surface of the beam in its damaged region with and end miller and a slide guide (Fig. 6a and b). The plates were pre-drilled with a specific template at the laboratory of the University of Brescia, thus providing the correct inclination of the holes within the plate thickness (Fig. 6c). Then, the steel plates were placed in each groove to be used as template to pre-drill the holes in the timber for the nailed connections (Fig. 6d). The grooves were cleaned with a brush and vacuum while the steel plates were sandblasted to ensure a satisfactory bond between the wood substrate and the steel plates. Finally, the epoxy-resin was applied to the steel plates and the groove sides and the nails were inserted into the holes (Fig 6e). It should be noted that the thixotropic properties of the epoxy-resin adhesive allowed the plates to be glued to the groove surfaces without requiring moulding or formwork. Several wedges were applied between each pair of bonded plates to guarantee the positioning of the plates and to provide pressure during the adhesion curing (Fig. 6f). Ten days after the repair, the props were removed from the floor and the repaired beam showed an instantaneous deflection of about 1.5 mm.

4. Experimental study on the delamination

4.1. Test set up

The proposed technique for the repair of timber beams was experimentally studied at the P. Pisa Laboratory of the University of Brescia with the aim of investigating the diffusive phenomena that can cause plate delamination. A larch beam (2.0 m long, 70 mm × 300 mm in cross section), repaired with two glued steel plates was tested. A notch (4 mm wide and 40 mm deep) was cut on the soffit and at the midspan of the beam to reproduce a splitting failure of a damaged beam (Fig. 7) The steel plates (3 × 30 mm in cross section) were designed to obtain the initial stiffness and the strength of the uncracked original beam, assuming, as in the ancient beam of Palazzo Calini, a maximum stress of 5 and 100 MPa for timber and steel under service conditions, respectively. An adhesive layer thickness of 1 mm on average was measured before testing [30].

The beam was tested supported over a span of 2 m and loaded at midspan. The test was carried out under displacement control by means of a mechanical jack. The load was measured by a load cell placed between the jack and the steel HE140A beam of the reacting steel bench, while the beam deflection was measured by three potentiometric transducers placed against the upper surface of the beam (position 1 at midspan, position 2 and position 3 and at the supports as shown in Fig. 7). The average displacement rate was very slow (0.05 mm/min) in order to accurately measure the onset of the plate delamination.

The diffusion phenomena at the plate ends or at the crack in the beam was investigated by means of the Moiré interferometry analysis. In the past the Moiré interferometry technique was used to study the flexural cracks of reinforced concrete beams or to study the slip-zone propagation at the bar-to-concrete interface in cracked concrete [34]. The Moiré grid method has the advantage of giving a complete displacement field in a single picture.

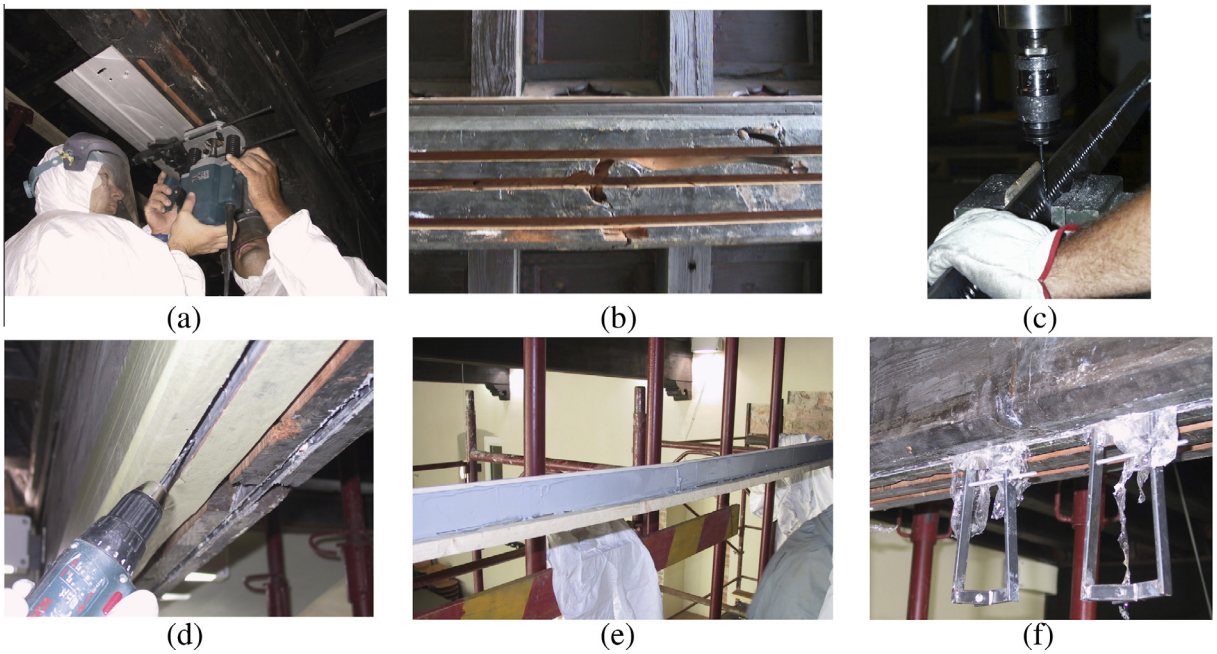

Fig. 6. Repair of the historical beam at Palazzo Calini ai Fiumi (Brescia, Italy): (a) beam notching with the end miller machine and the slide guide; (b) grooves before glueing of the reinforcements; (c) pre-drilling of the steel plates; (d) pre-drilling of the holes in the timber; (e) application of the adhesive on the steel plates; (f) wedges applied during adhesive curing.

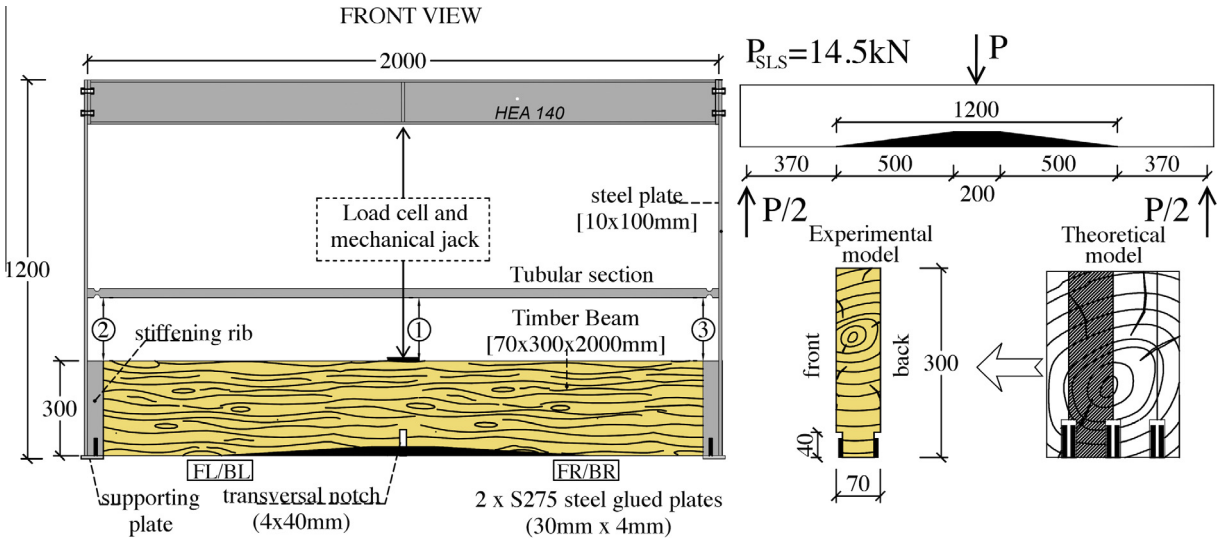

Fig. 7. Test set up and specimen characteristics.

Therefore, it can provide a great deal of refined data concerning the diffusion of local problems. In the test on the repaired timber beam, the analysis of the Moiré interferometry effects allowed the shear strain of the wood to be calculated in the zone of stress concentration around the plate ends or at the beam notch at midspan.

The Moiré fringes were obtained by superimposing two gratings with a density of 40 lines/mm. The first stripping grating was glued to the bottom surface of the timber beam with the lines oriented perpendicularly to the beam/plate axis, while a second grating (reference grating) was superimposed on the first with a thin layer of paraffin oil in between. Each relative movement between the first grating, which deforms like the beam's bottom surface, and the undeformed reference grating, generates Moiré fringes perpendicular to the monitored displacements. Owing to the differences in the pitch values of the two gratings, the initial fringe pattern (mismatch) was taken into consideration during the fringe processing. A difference of a fringe order corresponds to a longitudinal displacement (perpendicular to the grating lines) equal to 0.0254 mm. Thus, for a given applied load (P), the difference of fringe order between the timber fibre (Δn_t) and the steel plate axis (Δn_s) along a given directrix (x) at the distance (y) from the timber–glueing surface, provides the relative displacement (δ), as given by the following equations

$$\delta = (\Delta n_t - \Delta n_s)0.025 \text{ mm} \tag{8}$$

As a result, the shear local strain (γ) is given by (Fig. 8):

$$\gamma = \delta / y \tag{9}$$

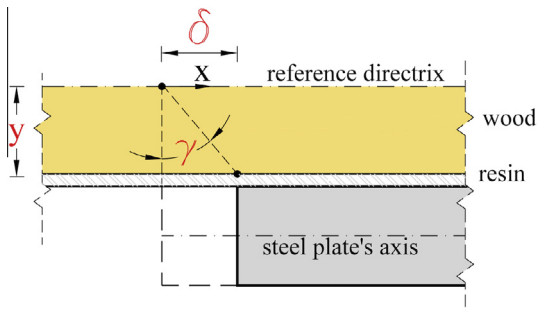

Fig. 8. Local timber shear deformation (γ) at the distance (y) from the glueing surface.

Furthermore, the discontinuity of the Moiré fringes allowed the load causing the onset of the delamination of the steel plate to be accurately measured. Further details of the test set-up and the collection of the fringe pattern pictures for each load increment taken at the plate ends and at beam midspan can be found in [30].

4.2. Test results

The global response of the tested repaired beam is described by the load–deflection curve (Fig. 9a). Five cycles were applied up to the service load (P_{SLS}) of 14 kN and then the load was increased up to the onset of the plate delamination. A linear elastic behaviour can be noted up to the plate delamination when the test was interrupted.

In Fig. 10a and b the Moiré interference effects for a load $P = 0$ kN (initial mismatch) and for a load $P = 22$ kN are shown. Fig. 10c shows the discontinuity of Moiré fringes for the load $P = 23$ kN, for which the onset of the delamination occurred at the left end of the plate placed on the beam's back side (labelled with position BL in Fig. 7). Finally, the load was kept constant at the peak value of 23 kN to monitor the propagation of the plate delamination. It rapidly moved forward within the first 8 h up to the distance of 8.0 mm away from the plate end at a rate of about 0.37 mm/h, while it stabilised after 24 h with a debonded length of 11 mm (Fig. 9b).

With regard to the wood strain measured using the Moiré technique, the results around the region at the left end of the back plate, where the delamination occurred (position BL/FL in Fig. 7), are presented. Further details of the measured wood strains close to the plate ends and to the notch at the beam midspan can be found in [30]. In Fig. 11a the shear strains of the wood evaluated along the longitudinal directrix (x) at a distance of 1 mm from the glued surface (as shown in Fig. 8) are plotted for increasing values of the applied load (P). For a load $P = 22$ kN, before the plate delamination occurred, the test results showed a remarkable value of the shear strain ($\gamma = 16 \times 10^{-3}$), far beyond the elastic limit (γ_{el}) of about 3×10^{-3} provided by the results of local shear tests on sapwood which can be found in the literature [31,35]. Furthermore, the shear strain of the wood remains in the elastic range ($\gamma < \gamma_{el}$) for a distance greater than 70 mm from the plate end.

In Fig. 11b the slip (δ) between the back plate's axis and the timber layer at distance (y) from the glued surface is plotted for a distance $x = 11.5$ and 22 mm from the left plate end at a load $P = 22$ kN

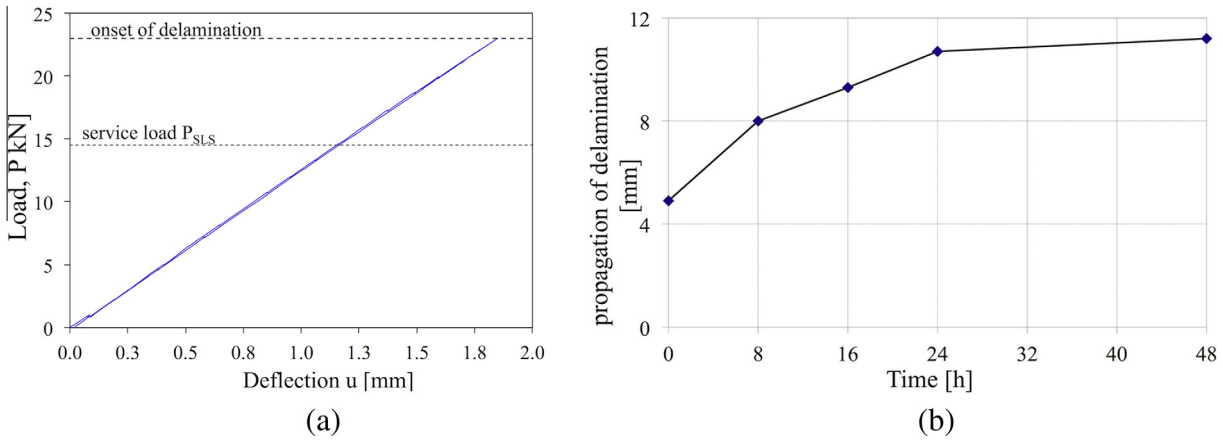

Fig. 9. Test results: beam deflection (a); propagation of plate delamination (b).

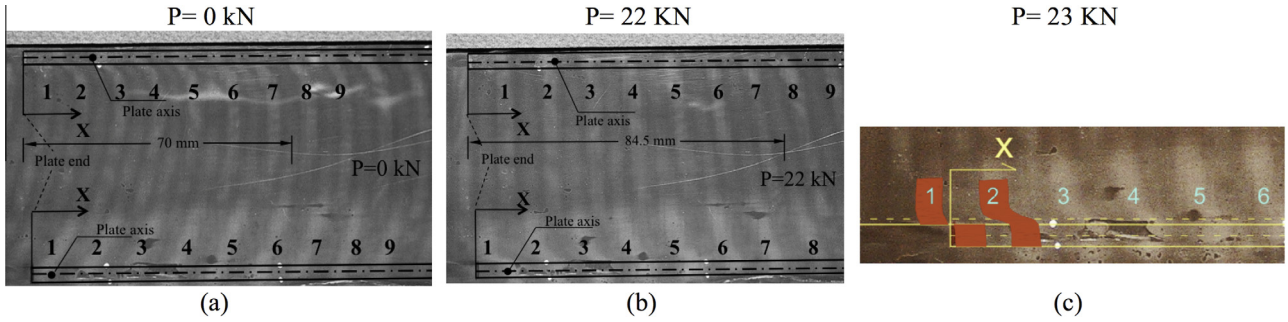

Fig. 10. Moiré interference effects for a load $P = 0$ kN (initial mismatch) (a), for $P = 22$ kN (b) and for the load $P = 23$ kN for which the plate delamination occurred (c).

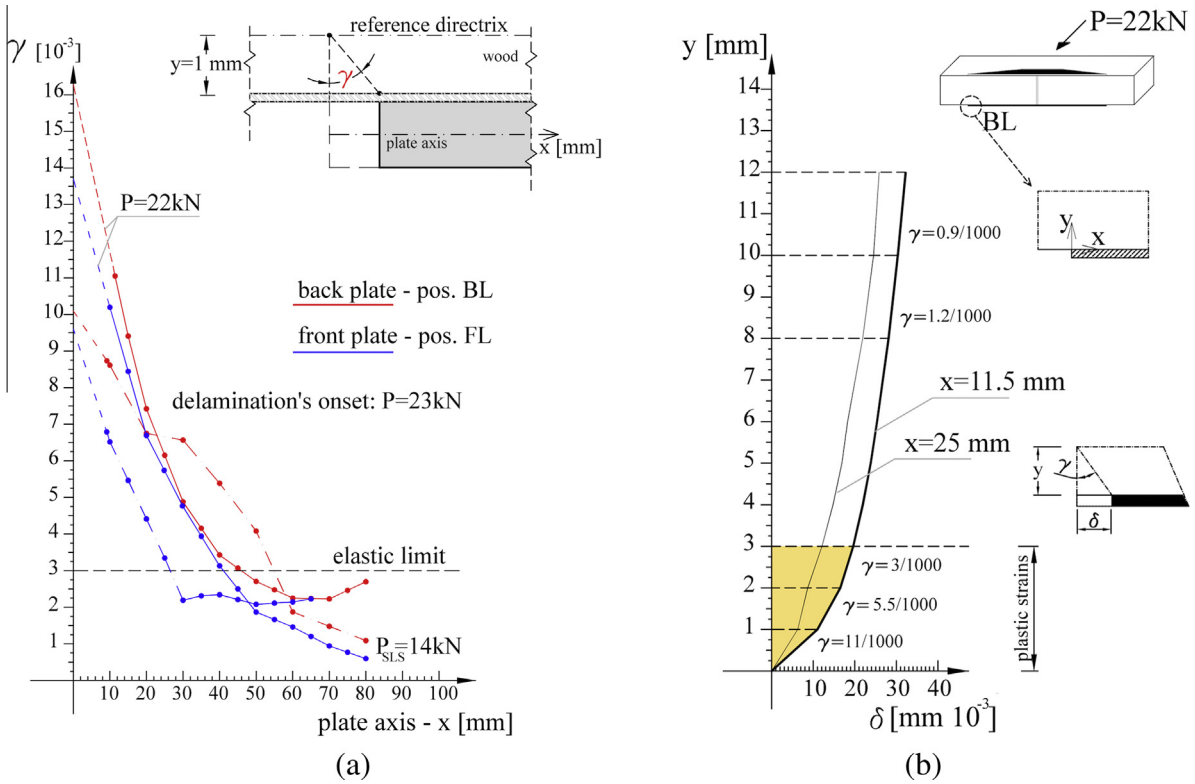

Fig. 11. Test results: wood shear deformation (γ) at the left plates's end evaluated at a distance equal to 1 mm from the timber–glue interface (a); slip (δ) between the plate and the timber fibres at a distance $x = 11.5$ or 22 mm from the left end of the back plate (position BL) (b).

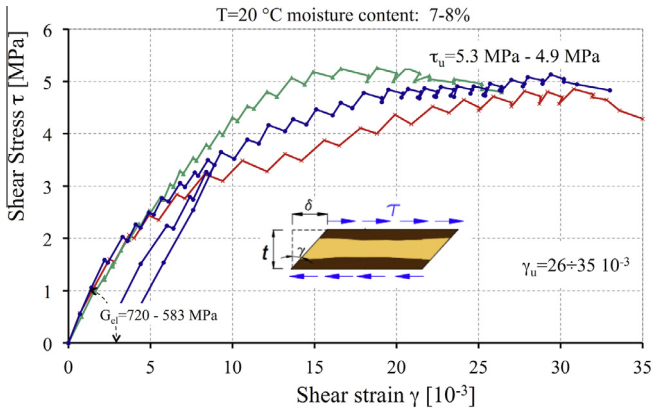

Fig. 12. Experimental shear (τ) versus strain (γ) curves for sapwood [31,36].

(slightly lower than the delamination load P_D = 23 kN). It should be noted that that the zone with a non-linear shear behaviour was localised in a very limited area, not farther than 3 mm from the glue–timber interface and that the stress diffusion effects fade out at a distance of about 10 mm form the glued surface.

This non-linear shear behaviour of the wood allows for the redistribution of shear stresses at the timber-reinforcement interface, thus mitigating the peak value of the stresses at the end plate and reducing the risk of its delamination. In fact, even though elastic finite element analyses may show a stress concentration able to delaminate the reinforcements already at the service load [30,35], the test results pointed out that the peeling crack onset occurred at a load equal to 1.64 times the service load (P_{SLS} = 14 kN). Therefore, the peeling phenomenon is governed by the local shear behaviour of sapwood and by its capability to develop plastic strain.

The results presented, evaluated by means of the Moiré technique, addressed a broad experimental campaign, carried out by Giuriani and Metelli [31,36], to provide an accurate shear stress–strain constitutive law for larch sapwood. It showed significant plastic behaviour with an ultimate shear strain (γ_u) up to the value of 35.0×10^{-3} corresponding to a shear strength of about 5.0 MPa (for a moisture content of 7%) (Fig. 12). These results can be considered an effective tool for numerical or analytical computation on shear stress concentration of bonded FRP or steel plates, which cannot be studied without taking into account the plastic resources of wood in shear [36].

5. Monitoring of the Palazzo Calini beams

The wooden floor of Palazzo Calini has been constantly monitored for fourteen years. Readings were taken periodically after TA beam repair, from September 2001 until August 2015. No data of deflection are available from the time of floor strengthening (1997) to the time of beam repair (2001). As shown in Fig. 13a, the deflection increase of the repaired beam (labelled TA-R) as well as of the two adjacent undamaged main beams (labelled TB and TC), the room temperature, the atmospheric relative humidity (Fig. 13b) and the moisture content of the repaired beam have also been measured. During the first year three readings per month were taken, in the second year the frequency was reduced to once per month, and after September 2003 the frequency was reduced further to three times per year. Readings were always taken at the same time of the day (in the morning hours around 10 am). The wood moisture content is evaluated by means of an electronic meter based on the electric resistance measurement principle.

More than fourteen years after the repair, the deflection of the repaired beam TA-R has increased by 7.23 mm. The deflection of the undamaged TB and TC beams has increased by 6.79 and 7.07 mm, respectively (Fig. 13a). It is worth noting all the three monitored beams have shown the same deflection increase, which confirms the effectiveness of the adopted technique to repair the damaged beam.

The collected data allow for a few considerations on the creep behaviour of the timber-to-concrete composite floor. It should be noted that the monitoring evidences a rather steadily deflection increase of the floor of Palazzo Calini (0.5 mm/year on average over 14 years). This phenomenon is due to the rheological behaviour of concrete slab, timber beam and timber-to-concrete slab connection adopted in the floor's stiffening intervention (on 1997), as well as to the mechano-sorptive creep of timber, induced by the moisture content variation [37].

From September 2001 to November 2008 the deflection of the all the floor beams was characterised by a mean increase of about 0.7 mm/year. During the same period, the room humidity varied between 22% and 68% while the room temperature varied from 18 to 28 °C (Fig. 13b). In Fig. 13a the plotted data show the cyclic variations of the beam deflection, with maximum amplitude of about 1.4 mm during the first year after the intervention, due to the seasonal cyclic variations of temperature and moisture content. The deflection increase of the floor of Palazzo Calini was likely influenced also by the mechano-sorptive creep behaviour of wood.

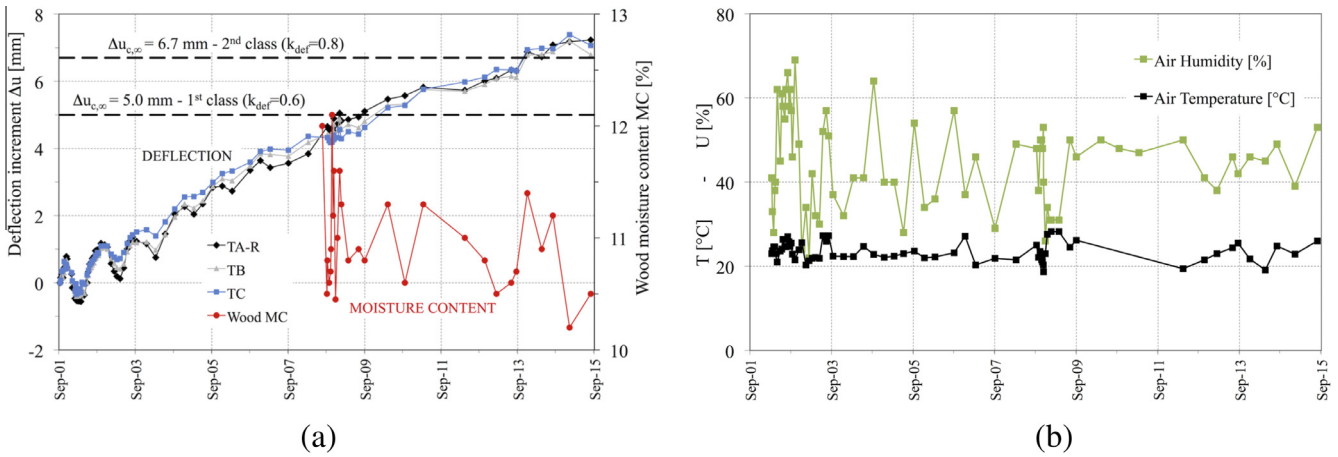

Fig. 13. Monitoring of the floor in Palazzo Calini (Brescia, Italy): deflection (from 2001 to 2015) and wood moisture content (from 2008) (a); room humidity and temperature (b).

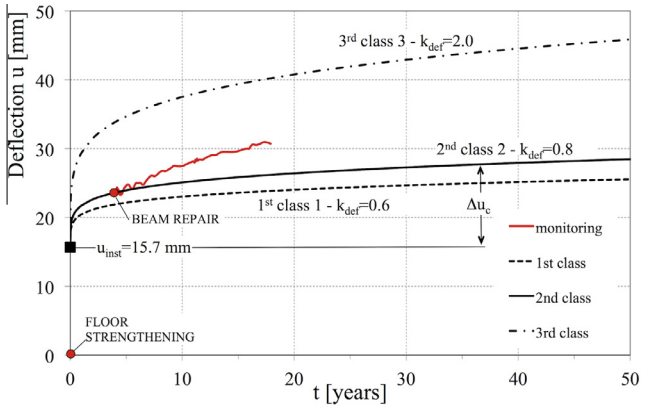

Fig. 14. The increase of midspan deflection with time of the timber-to-concrete composite beam: comparison between monitoring data (averaged value) and the long-term prediction according to Eurocode 5 [29].

This may be confirmed in Fig. 13b, which shows the several cyclic variations of room humidity recorded from September 2001 to November 2008. For this reason, on November 2008 an air humidifier was installed in the room in order to reduce the peak of air humidity variation. As a result, the wood moisture content was stabilised around a value of 11% and the beams' deflection increase was reduced to 0.35 mm/year over the last seven years.

In order to prove the important creep effect on floor deflection, the estimated final creep deflection increment ($\Delta u_{c,\infty}$) for a quasi-permanent combination of action (Eq. (6)) is shown in Figs. 13a and 14. The creep deflection is calculated with the simplified approach proposed in Annex B of Eurocode 5 [29] for composite beams with flexible connections. Similar accurate results can be obtained also by means of an exact relationship between the slope increment of the beam end and the maximum concrete–timber slip at the support [38–40]. The calculation is carried out by assuming a simple-supported beam, a linear elastic behaviour of all components (timber, concrete, connection), a modulus of concrete E_c = 31470 MPa [41], a modulus of elasticity of the wood E_w = 11500 MPa [25], a timber-to-concrete connection stiffness K_S = 22700 N/mm as proposed by Gelfi et al. [1] for connection with 16 mm stud diameter.

Effects of creep under sustained loads are accounted for by using the effective modulus method, namely by replacing the elastic moduli of concrete or timber (E) and the connection stiffness (K_s) with the effective moduli and effective stiffness, respectively:

$$E_{eff} = E/[1 + \phi(t_\infty; t_0)] \tag{10}$$

$$K_{s,eff} = K_s/[1 + \phi_s(t_\infty; t_0)] \tag{11}$$

where ϕ is the creep coefficient of the component material, t_∞ and t_0 are final and initial time of analysis, respectively. The creep coefficient of timber, denoted as k_{def}, is defined in Eurocode 5 [29] depending on the service class (i.e. moisture content of wood). It varies between 0.6 and 2.0. For the connection system, the creep coefficient is assumed twice as large as the creep coefficient of wood [39,40,42]. A final creep coefficient $\phi_c(t_\infty; t_0) = 2$ for concrete can be assumed, according to the model in Annex B of Eurocode 2 [41]. The proposed procedure neglects effects of concrete shrinkage and inelastic strains of concrete and timber due to thermo-hygrometric environmental variations, as suggested also in the literature for simplified methods [42].

Finally, in Fig. 14 the trend of the predicted beam deflection over 50 years is shown for different environmental conditions. The trends in time of the beam deflection were qualitatively evaluated by approximating the creep coefficient previously defined by a power-type relationship from the initial to the final time of analysis [37,42].

Despite the uncertainties due to the material properties, missing data of the moisture content and beam deflection during the first four years after the floor strengthening as well as to the simplicity of the adopted creep model, it should be noted that the estimated deflection is consistent with the monitoring results. It appears that the use of the coefficient tabled for the 2nd service class leads to the best approximation of the recorded deflections since the air humidity showed higher seasonal fluctuation with peaks greater than 65% during the first years after the floor strengthening, until the installation of the air humidifier on 2008. This could have caused moisture content of the timber exceeding 12%. The model underestimates the deflection by about 16% at eighteen years since floor strengthening (Fig. 14). However, the analytical–experimental comparison confirms the difficulties to choose the proper creep coefficient, even in an indoor environment, since the phenomenon is governed by several parameters whose influence is still difficult to be correctly evaluated (cyclic variation of the moisture content [37] and the value of stress in the timber joists under service condition [43]).

Furthermore, on the basis of the result of the analytical calculation floor would exhibit a significant final deflection of about 26 and 29 mm ($\approx L/300$) for 1st and 2nd service class, respectively, after 50 years since the strengthening intervention (Fig. 14). The final deflection could be 1.8 times the instantaneous deflection (u_{inst} = 15.7 mm) for 2nd service class. This result is mainly related to the high timber stress in the composite beams under service condition. The timber stress is 9.0 and 8.0 MPa for the rare and quasi-permanent load combination of actions, respectively, thus confirming that the creep phenomena may be significant when the timber stress is greater than 4 ÷ 5 MPa for dead loads only under service condition [43]. It should be also noted that from 1997 to 2001 (during this period the deflection was not monitored) the beams could have exhibited almost 55% of the overall creep deflection, which is about 10 and 13 mm for 1st and 2nd service class, respectively.

In conclusion, the final creep deflection, albeit rather high, seems to stabilize as it can be confirmed both by the analytical model and by the recorded deflection, if its seasonal fluctuations are neglected.

6. Concluding remarks

In this paper a non-invasive technique for the repair of wooden floors is presented. An ancient larch beam in the floor of the 15th century Palazzo Calini (Brescia, Italy) was repaired using steel plates bonded on one side only in longitudinal grooves in order to allow the free swelling and shrinkage of the wood in the direction transversal to the gluing surface, thus reducing the risk of plate delamination. Furthermore, a set of high strength steel nails was forced into calibrated holes to guarantee the transmission of the load from the steel plates to the wooden beam in case of loss of adhesion (fire or delamination). Continuous monitoring of the wooden floor confirms the effectiveness of the adopted technique, as the repaired beam has showed the same deflection increment of the undamaged beams since beam repair.

The adopted technique requires particular attention to the delamination of the glued plates due to the shear and normal stress concentrations, which occurs at the end of the repairing element. This phenomenon was studied experimentally by means of the Moiré interferometry analysis on a larch beam with a crack at the midspan and reinforced with two glued steel plates. The results showed that the capability of sapwood to develop shear plastic strains reduces the risk of plate debonding under service loads,

as the onset of the plate delamination occurred at a load equal to 1.64 times the service load and with a shear strain of sapwood much greater than the elastic limit.

Finally, even though floor monitoring aims at checking the plate delamination in the repaired beam, it provides supplementary information regarding the long-term behaviour of the timber-to-concrete composite floor. Fourteen years after the repair of the damaged beam, the beams have showed a rather high deflection increase of about 7 mm (0.5 mm/year). This phenomenon is due the creep effects of timber, which depend mainly on permanent loads and on the moisture content of timber, which also fluctuated during the early years after floor strengthening. An analytical estimation of the long-term deflection based on the procedure of Eurocode 5 [29] suggests that the floor may be assigned to the 2nd service class.

Acknowledgements

The authors also gratefully acknowledge Mr. Domenico Fiorillo and Eng. Egidio Marchina of the P. Pisa Laboratory of the University of Brescia for their technical support during the timber beam repair and monitoring in Palazzo Calini (Brescia, Italy).

References

[1] P. Gelfi, E. Giuriani, A. Marini, Stud shear connection design for composite concrete slab and wood beams, J. Struct. Eng. 128 (12) (2002) 1544–1550, http://dx.doi.org/10.1061/(ASCE)0733-9445.
[2] M. Piazza, G. Turrini, A technique for the restoration of timber floors, Recuperare 5–7 (1983) (in Italian).
[3] G. Tampone, The structural rehabilitation of timber floors by means of steel plates in Genio Civile Building – Florence, in: Proceedings of the 2° National Congress "Wood Restoration", 8–11 November 1989, vol. 1, Florence, Italy, pp. 263–281 (in Italian).
[4] J. Peterson, Wood beams prestressed with bonded tension elements, J. Struct. Div. ASCE 91 (1) (1965) 103–119.
[5] K.B. Borgin, G.F. Loedolff, G.R. Saunders, Laminated wood beams reinforced with steel strips, J. Struct. Div. ASCE 94 (71) (1958) 596–602.
[6] J. Jasieńko, T.P. Nowak, Solid timber beams strengthened with steel plates – experimental studies, Constr. Build. Mater. 63 (2014) 81–88, http://dx.doi.org/10.1016/j.conbuildmat.2014.04.020.
[7] U. Meier, Strengthening of structures using carbon fibre/epoxy composites, Constr. Build. Mater. 9 (6) (1995) 341–351, http://dx.doi.org/10.1016/0950-0618(95)00071-2.
[8] F.W. Kropf, U. Maierhofer, Strengthening, retrofitting and upgrading of timber structures with high-strength fibres, Struct. Eng. Int. 10 (3) (2002) 178–181.
[9] T.C. Triantafillou, N. Deskovic, Prestressed FRP sheets as external reinforcement of wood members, J. Struct. Eng. 118 (5) (1992) 1270–1285.
[10] A. Borri, M. Corradi, A. Grazini, A method for flexural reinforcement of old wood beams with CFRP materials, Composites 36 (2) (2005) 143–153, http://dx.doi.org/10.1016/j.compositesb.2004.04.013.
[11] L.L. Jankowski, J. Jasieńko, T.P. Nowak, Experimental assessment of CFRP reinforced wooden beams by 4-point bending tests and photoelastic coating technique, Mater. Struct. 43 (1) (2010) 141–150, http://dx.doi.org/10.1617/s11527-009-9476-0.
[12] C. Gentile, D. Svecova, S.H. Rizkalla, Timber beams strengthened with GFRP bars: development and applications, J. Compos. Constr. 6 (1) (2002) 11–20, http://dx.doi.org/10.1061/(ASCE)1090-0268(2002) 6:1(11).
[13] H. Alhayek, D. Svecova, Flexural stiffness and strength of GFRP-reinforced timber beams, J. Compos. Constr. 16 (2012) 245–252, http://dx.doi.org/10.1061/(ASCE)CC.1943-5614.0000261.
[14] P. Alam, M.P. Ansell, D. Smedley, Mechanical repair of timber beams fractured in flexure using bonded-in reinforcements, Compos. B 40 (2009) 95–106, http://dx.doi.org/10.1016/j.compositesb.2008.11.010.
[15] R.N. Swamy, R. Jones, J.W. Bloxham, Structural behaviour of reinforced concrete beams strengthened by epoxy-bonded steel plates, Struct. Eng. 65A (2) (1987) 59–68.
[16] D.J. Oehlers, J.P. Moran, Premature failure of externally plated reinforced concrete beams, J. Struct. Eng. 116 (4) (1990) 978–995.
[17] H. Rahimi, A. Hutchinson, Concrete beams with externally bonded FRP plates, ASCE JCC 5 (1) (2001) 44–56, http://dx.doi.org/10.1061/(ASCE)1090-0268(2001) 5:1(44).
[18] W.M. Sebastian, Significance of midspan debonding failure in FRP-plated concrete beams, ASCE J. Struct. Eng. 127 (7) (2001) 792–798, http://dx.doi.org/10.1061/(ASCE)0733-9445(2001) 127:7(792).
[19] J.G. Teng, J.W. Zhang, S.T. Smith, Interfacial stress in reinforced concrete beams bonded with a soffit plate: a finite element analysis, Constr. Build. Mater. 16 (1) (2002) 1–14, http://dx.doi.org/10.1016/S0950-0618(01)00029-0.
[20] M. Malek, H. Saadatmanesh, R. Ehsani, Prediction of failure load of R/C beams strengthened with FRP plate due to stress concentration at the plate end, ACI Struct. J. 95 (1) (1998) 142–152.
[21] E. Cosenza, M. Pecce, Shear and normal stresses interaction in coupled structural system, J. Struct. Eng. 127 (1) (2001) 84–88, http://dx.doi.org/10.1061/(ASCE)0733-9445(2001) 127:1(84).
[22] S.T. Smith, J.G. Teng, FRP-strengthened RC beams. II: assessment of debonding strength models, Eng. Struct. 24 (4) (2002) 397–417, http://dx.doi.org/10.1016/S0141-0296(01)00106-7.
[23] R. Wong, F.J. Vecchio, Towards modeling of reinforced concrete members with externally bonded fiber-reinforced polymer composites, ACI Struct. J. 100 (1) (2003) 47–55.
[24] A. Aprile, E. Spacone, S. Limkatanyu, Role of bond in RC beams strengthened with steel and FRP plates, J. Struct. Eng. 127 (12) (2001) 1445–1452, http://dx.doi.org/10.1061/(ASCE)0733-9445(2001) 127:12(1445).
[25] UNI 11035-2:2010, Legno strutturale Regole per la classificazione a vista secondo la resistenza meccanica e valori caratteristici per i tipi di legname strutturale italiani (in Italian).
[26] EN 1991-1-1:2002, Eurocode 1 – actions on structures - Part 1–1: general actions – densities, self-weight, imposed loads for buildings, Brussels, Belgium: CEN, European Committee for Standardization.
[27] E. Giuriani, A. Gubana, A penetration test to evaluate wood decay and its application to the loggia monument, Mater. Struct. 26 (1993) 8–14.
[28] EN 1990:2002+A1:2005, Eurocode – basis of structural design, CEN, European Committee for Standardization, Brussels, Belgium.
[29] EN 1995-1-1:2004+A2:2014, Eurocode 5 – design of timber structures Part 1–1: General-common rules and rules for building, CEN, European Committee for Standardization, Brussels, Belgium.
[30] G. Metelli, Coupling problem in the structural repair and strengthening (Ph.D. thesis), Supervisor: Prof. E. Giuriani, University of Brescia, Italy, 2003 (in Italian).
[31] E. Giuriani, G. Metelli, The role of sapwood plasticity in the delamination phenomenon of repaired timber beams, Int. J. Restor. 10 (4) (2004) 317–334.
[32] K.W. Johansen, Theory of timber connections, International Association of Bridge and Structural Engineering, Publication 9, Bern, IABSE, 1949, pp. 249–262.
[33] F. Germano, G. Metelli, E. Giuriani, Experimental results on the role of sheathing-to-frame and base connections of a European timber framed shear wall, Constr. Build. Mater. 80C (2015) 315–328, http://dx.doi.org/10.1016/j.conbuildmat.2015.01.076.
[34] E. Giuriani, P. Gelfi, The slip-zone propagation at the bar-to-concrete interface in cracked concrete (in Italian), Stud. Res. 4 (1982) 57–83.
[35] K.B. Dahl, K.A. Malo, Nonlinear shear properties of spruce softwood: experimental results, Wood Sci. Technol. 43 (7–8) (2009) 539–558, http://dx.doi.org/10.1007/s00226-009-0247-4.
[36] G. Metelli, E. Giuriani, E. Marchina, The repair of timber beams with controlled-debonding steel plates, in: Advanced Materials Research 2013, vol. 778, pp. 588–595, 2nd International Conference on Structural Health Assessment of Timber Structures, Trento, 4th–6th September 2013. doi:10.4028/www.scientific.net/AMR.778.588.
[37] T. Toratti, Creep of Timber Beams in a Variable Environment, Helsinki Univ. of Technology, Helsinki, Finland, 1992. Rep. No. 31.
[38] P. Gelfi, E. Giuriani, Influence of slab-beam slip on the deflection of composite beams, Int. J. Restor. Build. Monuments 9 (5) (2003) 475–490. Aedificatio Verlag, ISSN 0947-4498.
[39] P. Gelfi, A. Marini, Solai misti legno calcestruzzo: metodi di verifica (prima parte). L'Edilizia, vol. 153, 2008, pp. 44–51, ISSN: 1593-3970 (in Italian).
[40] P. Gelfi, A. Marini, Solai misti legno calcestruzzo: metodi di verifica (seconda parte) L'Edilizia, vol. 154, 2008, pp. 26–31, ISSN: 1593-3970 (in Italian).
[41] EN 1992-1-1:2004, Eurocode 2 – design of concrete structures. Part 1–1: general rules and rules for buildings, CEN, European Committee for Standardization, Brussels, Belgium.
[42] A. Ceccotti, M. Fragiacomo, S. Giordano, Long-term and collapse tests on a timber concrete composite beam with glued-in connection, Mater. Struct. 40 (1) (2006) 15–25, http://dx.doi.org/10.1617/s11527-006-9094-z.
[43] E. Giuriani, Consolidamento degli edifici storici. Ed Utet, Torino (Italy), 2012. ISBN: 978-88-598-0763-6 (in Italian).